# A novel model for the first nucleotide binding domain of the cystic fibrosis transmembrane conductance regulator

Jean-Philippe Annereau[a], Ulrich Wulbrand[b], Anne Vankeerberghen[c], Harry Cuppens[c], François Bontems[a], Burkhard Tümmler[b], Jean-Jacques Cassiman[c], Véronique Stoven[a,*]

[a]*Laboratoire de RMN, DCSO, Ecole Polytechnique, 91128 Palaiseau Cedex, France*
[b]*Klinische Forschergruppe, Medizinische Hochschule, D-30623 Hannover, Germany*
[c]*Center for Human Genetics, KU, Leuven, Belgium*

Received 14 February 1997; revised version received 20 March 1997

**Abstract Cystic fibrosis is caused by mutations in the cystic fibrosis transmembrane conductance regulator (CFTR) gene. The most frequent mutation is the deletion of F508 in the first nucleotide binding fold (NBF1). It induces a perturbation in the folding of NBF1, which impedes posttranslational maturation of CFTR. Determination of the three-dimensional structure of NBF1 would help to understand this defect. We present a novel model for NBF1 built from the crystal structure of bovine mitochondrial $F_1$-ATPase protein. This model gives a reasonable interpretation of the effect of mutations on the maturation of the protein and, in agreement with the CD data, leads to reconsideration of the limits of NBF1 within CFTR.**



*Key words:* Cystic fibrosis transmembrane conductance regulator; Nucleotide binding fold; Model building; Cystic fibrosis; Circular dichroism; ABC transporter

## 1. Introduction

Cystic fibrosis (CF) is a frequent genetic disease caused by mutations in the CF gene. This gene encodes the cystic fibrosis transmembrane conductance regulator (CFTR), a 1480 amino acid transmembrane protein which functions as a $Cl^-$ channel. CFTR belongs to the phylogenetically ancient ABC transporters which constitute the largest family of paralogous proteins in prokarya, archaea and eukarya [1]. It was predicted to present two membrane spanning domains, a regulatory R domain, and two nucleotide binding folds (NBF1 and NBF2) [2]. The most frequent CF causing mutation is a deletion in NBF1 (ΔF508). This deletion probably induces a perturbation in the folding of NBF1, and consequently impedes CFTR from posttranslational maturation [3]. Therefore, knowledge of the three-dimensional (3D) structure of NBF1 would help to understand the effect CF mutations. In the absence of a known defined structure, we propose a new model for NBF1, built from the recently available X-ray structure of bovine mitochondrial $F_1$-ATPase protein [4], the only protein of known structure in the ABC family. We will show that this novel model facilitates the description of mutant phenotype in molecular terms.

## 2. Building of the model

### 2.1. Choice of the reference structure

The choice of a relevant reference structure expected to have the same global fold is a critical step in order to build a reliable model for NBF1. NBF1 of CFTR belongs to the superfamily of P-loop (also called Walker A) containing proteins which present α/β structures (or Rossman folds), consisting of a central β-sheet surrounded by helices on both sides. Based on the topology of the β-sheets, this superfamily is divided into four structural families [5]: 'kinases' such as adenylate kinase (ADK) [6], 'G proteins' such as p21-Ras [7] or elongation factor Tu [8], 'nitrogenase iron protein-like', and 'recA protein-like' such as $F_1$-ATPase, according to the SCOP structural data bank [5]. The 3D structure of ADK was chosen to build models for the NBF1 of CFTR because at that time no 3D structure of a representative member of the ABC family was known [1,9]. However, ADK and NBF1 are two evolutionarily quite unrelated molecules, indicated by the low overall sequence similarity (approximately 12% sequence similarity in conserved regions).

Recently the 3D structure of the $I_1$ domain of the $F_0F_1$-ATPase was resolved [4], which shares higher sequence similarity with NBF1, as shown below. Therefore we chose $F_1$-ATPase as reference structure for model building of NBF1, in which both the α and β subunits of $F_1$-ATPase (referred as NBFα and NBFβ in the following) were used, to exploit all the information for model building.

### 2.2. Strategy for building the model

*2.2.1. Sequence alignment and determination of conserved regions.* First, the backbones of NBFα and NBFβ were superimposed and graphically analyzed to identify the conserved regions where the main chains match, and the non-conserved regions where the main chains diverge. The alignment of NBF1 with NBFα and NBFβ was based on the optimal match between known secondary structure elements in NBFα and NBFβ and predicted in NBF1 by the PHD method (Profile fed neural network systems from Heidelberg) [10] and consensus motifs in the ABC family (Walker A, Walker B and C motifs) [11]. Insertions and deletions were introduced into non-conserved loops. The final sequence alignment is given in Fig. 1. According to this alignment NBF1 has approximately 28% sequence similarity with NBFα and NBFβ in conserved regions, which is significantly higher than its sequence similarity with ADK.

*2.2.2. Structural constraints.* In the conserved regions, conserved atoms were defined by the match in both the backbone and the side chains in NBFα, NBFβ and NBF1. Distances between all conserved atoms were calculated in NBFα and NBFβ, only short range distances being retained as constraints [12].

All possible φ, ψ and $\chi_1$ dihedral angles that could be deduced from the conserved atoms were calculated in NBFα

*Corresponding author. Fax: (33) 1-69-33-30-10.


*PII* S0014-5793(97)00363-3

and NBFβ, and introduced as dihedral constraints [12]. In case of diverging side chains in NBFα and NBFβ, and for residues situated in non-conserved loops, a $\chi_1$ value corresponding to the most probable rotamer was taken as initial value, with a tolerance of ± 30° [13]. A total of 10 800 distance and 355 dihedral constraints were used as geometrical restraints.

*2.2.3. Computation of the model.* The above constraints were used as input for distance-geometry calculations to compute structures using a standard procedure with the DIANA software [14,15]. Structures were refined to release all stress by simulated annealing using the X-PLOR software [16]. During this refinement step, improvement of the Ramachandran diagram for residues of non-conserved loops was obtained by applying an attraction potential towards allowed regions of the Ramachandran diagram [12–17].

### *2.3. Description and implications of the model*

The model for the NBF1 domain of human CFTR is shown in Fig. 2 (codons 453–650). It contains a central open twisted 6 stranded β-sheet (strands L453-G458, N505-S511, N538-G542, D567-D572, R600-V603, D614-I618) that alternate with 6 α-helices (K464-E474, Y517-D529, Q552-Y563, L581-V591, S605-K611, S631-L636), which constitutes a global Rossman fold. In Fig. 2, strands are labelled S1–S6 and helices H1–H6. The most C-terminal extended strand (K643-D648) is associated to strand 6, antiparallel to the other strands, and is labelled S7 in Fig. 2. F508 is situated in strand 2 of the central hydrophobic β-sheet, as shown in Fig. 2. Its deletion should destabilize the central β-sheet and impair folding presumably by a perturbation of the hydrophobic collapse stage. The previous models based on ADK placed F508 in peripheral regions, and therefore could not predict the deleterious impact of ΔF508 on protein folding.

In the model, the LSGGQ motif (or 'C motif') conserved among ABC transporters is situated at the surface of the domain which is consistent with its role to trigger interactions with other domains [18] of CFTR.

Moreover, the model leads to a reconsideration of the limits of NBF1 within the CFTR sequence. The N-terminal residue was initially defined by F434 and the C-terminal residue by I586, which is the terminal codon of exon 12. The whole exon 13 was thought to encode the regulatory R domain [19]. However, the size of a domain should be defined by the necessary secondary elements that guarantee folding integrity. According to the present model, NBF1 should extend to residue F650, i.e. by more than 60 residues into the region previously attributed to the regulatory R domain. This shift of the domain boundary is supported by sequence alignment with ABC transporters of other topologies, ending by an NBF domain at the C-terminus [20]. For example, the NBF domain of the ComA protein (the putative *Streptococcus pneumoniae* competence factor transporter) was aligned using the same method as for NBF1, as shown in Fig. 1. The alignment of NBF1 and NBF of ComA also ends close to residue F650.

## 3. Confrontation of the model with experimental data

### *3.1. Analysis of exon 13 CFTR mutants*

After translation, the wild-type CFTR protein (130 kDa) matures, through different glycosylation steps, from a core-glycosylated protein (150 kDa) in the endoplasmic reticulum (ER) to a mature protein (190 kDa) in the trans-Golgi [21]. Only the mature form will reach the cell membrane to form a functional chloride channel [22]. Some missense mutations or deletions, located in the CFTR coding region, result in a protein that only matures to the core-glycosylated form [23–25]. These mutations seem to interfere with the folding pattern of the CFTR protein, which results in their degradation at the level of the ER [26]. The maturation patterns of six mutant R domain proteins were determined (Fig. 3): CFTR-L610S, CFTR-G628R and CFTR-L633P matured to the core-glycosylated form, while CFTR-D648V, CFTR-T665S and CFTR-R766M matured to the complete glycosylated form. These results would indicate that the R domain might be divided into two domains. Amino acids located in the first domain (amino acids 610–633) play an important role in the folding of the polypeptide since, after mutagenesis of these amino acids, the resulting protein is recognized and retained by the control system that operates in the ER, while missense mutations located in the second domain (648–766) seem to have no effect on maturation. Preliminary results on a total of 16 different missense mutations in the R domain confirm this differential effect of mutations in the two R domain sequences [27]. These results are consistent with the assumption that the first part of the R domain is in fact the C-terminal part of NBF1.

### *3.2. CD spectroscopy*

Since ADK has been used previously to build a model for the NBF of ABC transporters [1], the validity of this approach may be tested by evaluation of the secondary structure profiles of NBF1 and ADK by CD spectroscopy.

The heterologously expressed NBF1 construct encompasses the complete sequence from the initially defined boundaries of the transmembrane to the regulatory domains [28]. As shown in Table 1, bundles of α-helices were found to be the major components in both NBF1 and ADK at pH 6–7 and low ionic strength. However, the susceptibility of secondary structure to pH and ATP was different in the two proteins. Loss of α-helix and increase of random coil was observed for NBF1 when pH was shifted from pH 7 to pH 8, whereas a similar change in ADK required the more alkaline pH 9 (Table 1). The most striking difference between NBF1 of CFTR and ADK was seen when the concentration of ATP was varied at pH 8 between 0 and 4 mM (Table 1). Secondary structure of ADK was insensitive to ATP. In the case of NBF1, however, the addition of low concentrations of ATP induced a gain of β-sheet structure and compensatory loss of random coil. When the concentration of ATP was further increased to 4 mM, α-helical contents of NBF1 dropped below 10% (Table 1). These data suggest that NBF1 structure is strongly influ-

→

Fig. 1. Sequence alignment of NBFα and NBFβ of $F_1$-ATPase, NBF1 of CFTR, and NBF of ComA. Positions of α-helices (known in NBFα and NBFβ and predicted in NBF1 and NBF of ComA) are indicated by striped bars, while β-sheets (also known in NBFα and NBFβ and predicted in NBF1 and NBF of ComA) are indicated by gray bars. Conserved regions are boxed.

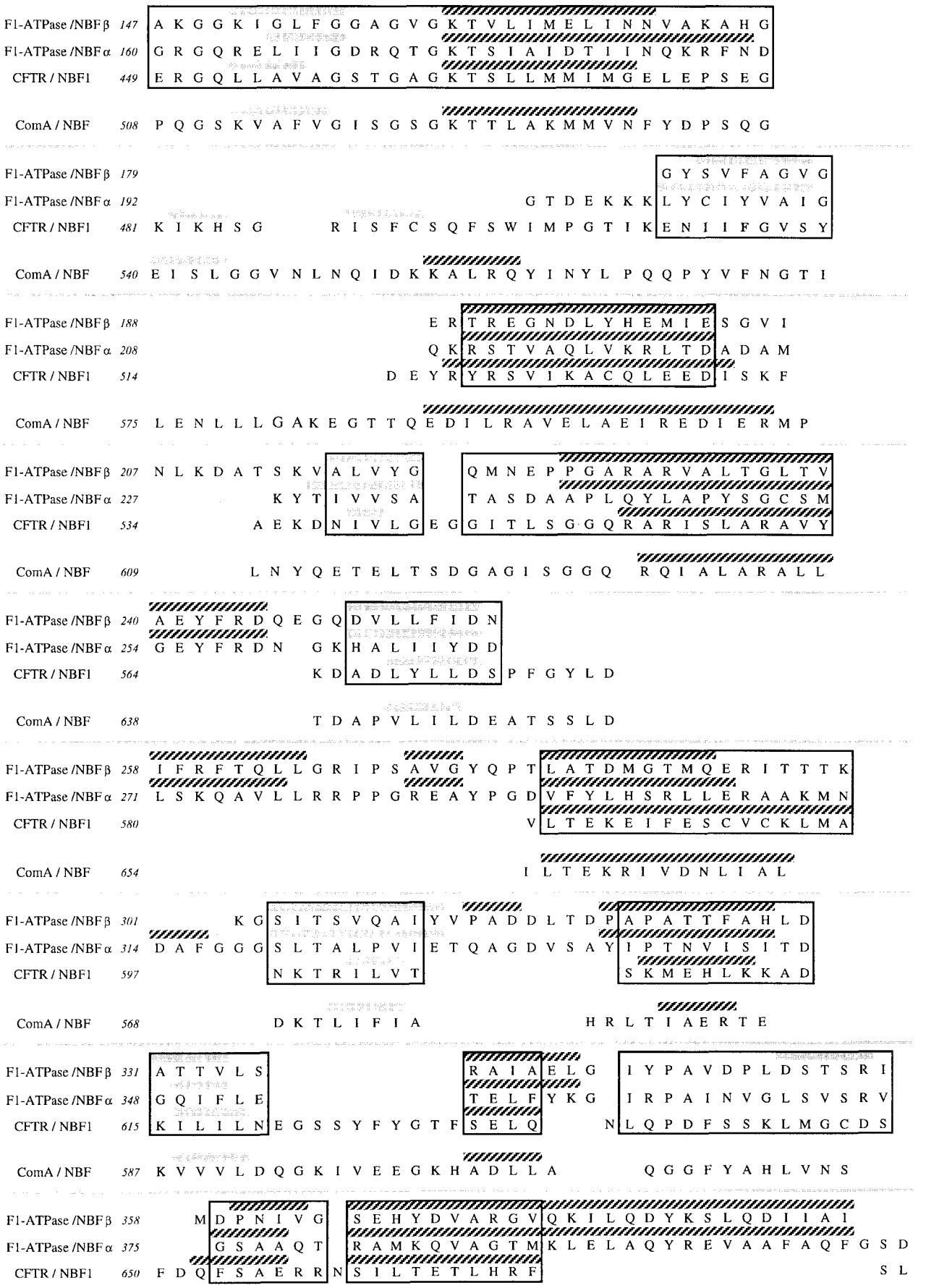
F1-ATPase /NBFβ 147 A K G G K I G L F G G A G V G K T V L I M E L I N N V A K A H G
F1-ATPase /NBFα 160 G R G Q R E L I I G D R Q T G K T S I A I D T I I N Q K R F N D
CFTR / NBF1 449 E R G Q L L A V A G S T G A G K T S L L M M I M G E L E P S E G
ComA / NBF 508 P Q G S K V A F V G I S G S G K T T L A K M M V N F Y D P S Q G
F1-ATPase /NBFβ 179 G Y S V F A G V G
F1-ATPase /NBFα 192 G T D E K K K L Y C I Y V A I G
CFTR / NBF1 481 K I K H S G R I S F C S Q F S W I M P G T I K E N I I F G V S Y
ComA / NBF 540 E I S L G G V N L N Q I D K K A L R Q Y I N Y L P Q Q P Y V F N G T I
F1-ATPase /NBFβ 188 E R T R E G N D L Y H E M I E S G V I
F1-ATPase /NBFα 208 Q K R S T V A Q L V K R L T D A D A M
CFTR / NBF1 514 D E Y R Y R S V I K A C Q L E E D I S K F
ComA / NBF 575 L E N L L L G A K E G T T Q E D I L R A V E L A E I R E D I E R M P
F1-ATPase /NBFβ 207 N L K D A T S K V A L V Y G Q M N E P P G A R A R V A L T G L T V
F1-ATPase /NBFα 227 K Y T I V V S A T A S D A A P L Q Y L A P Y S G C S M
CFTR / NBF1 534 A E K D N I V L G E G G I T L S G G Q R A R I S L A R A V Y
ComA / NBF 609 L N Y Q E T E L T S D G A G I S G G Q R Q I A L A R A L L
F1-ATPase /NBFβ 240 A E Y F R D Q E G Q D V L L F I D N
F1-ATPase /NBFα 254 G E Y F R D N G K H A L I I Y D D
CFTR / NBF1 564 K D A D L Y L L D S P F G Y L D
ComA / NBF 638 T D A P V L I L D E A T S S L D
F1-ATPase /NBFβ 258 I F R F T Q L L G R I P S A V G Y Q P T L A T D M G T M Q E R I T T T K
F1-ATPase /NBFα 271 L S K Q A V L L R R P P G R E A Y P G D V F Y L H S R L L E R A A K M N
CFTR / NBF1 580 V L T E K E I F E S C V C K L M A
ComA / NBF 654 I L T E K R I V D N L I A L
F1-ATPase /NBFβ 301 K G S I T S V Q A I Y V P A D D L T D P A P A T T F A H L D
F1-ATPase /NBFα 314 D A F G G G S L T A L P V I E T Q A G D V S A Y I P T N V I S I T D
CFTR / NBF1 597 N K T R I L V T S K M E H L K K A D
ComA / NBF 568 D K T L I F I A H R L T I A E R T E
F1-ATPase /NBFβ 331 A T T V L S R A I A E L G I Y P A V D P L D S T S R I
F1-ATPase /NBFα 348 G Q I F L E T E L F Y K G I R P A I N V G L S V S R V
CFTR / NBF1 615 K I L I L N E G S S Y F Y G T F S E L Q N L Q P D F S S K L M G C D S
ComA / NBF 587 K V V V L D Q G K I V E E G K H A D L L A Q G G F Y A H L V N S
F1-ATPase /NBFβ 358 M D P N I V G S E H Y D V A R G V Q K I L Q D Y K S L Q D I I A I
F1-ATPase /NBFα 375 G S A A Q T R A M K Q V A G T M K L E L A Q Y R E V A A F A Q F G S D
CFTR / NBF1 650 F D Q F S A E R R N S I L T E T L H R F S L

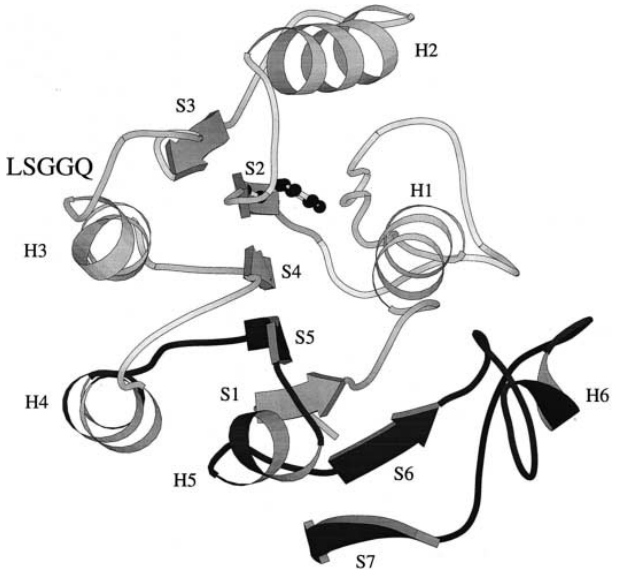


Fig. 2. Model for the NBF1 domain. Residues belonging to the NBF1 domain as initially defined (up to residue I586) are represented in gray. Residues belonging to the R domain as initially defined (starting at residue F587) are represented in black. Helices and sheets are labelled H1–H6 and S1–S7 respectively. The F508 residue side chain is shown by a ball-and-stick representation. The LSGGQ sequence is labelled and is exposed at the surface of the domain. This figure was drawn using the program MOLSCRIPT [32].

enced by ATP and that at least three different conformations exist at zero, low and high ATP concentrations, which is not expected for a globular folded protein. This differential response of NBF1 and ADK to pH and ATP suggests that either NBF1 (in its initial boundaries) represents a truncated domain or/and NBF1 and ADK do not share the same secondary structure characteristics.

## 4. Conclusion

The structural and functional studies of NBF1 of the CFTR protein presented here suggest that the structural model initially proposed for this domain might not be adequate. In contrast, our novel structural model based on the homology of NBF1 with NBFα/β of $F_1$-ATPase appears to provide a better fit between the structural and functional studies. This model also gives a more reasonable interpretation of the effect of mutations on the maturation of the proteins. Indeed, the majority of the mutations in the NBF1, including those in the first part of the domain previously considered to be the R domain, appear to result in premature degradation of the CFTR protein. Moreover, the comparison of the CD data of NBF1 and ADK shows that there is a contradiction between the initial definition of NBF1 and a kinase global fold.

Further modeling of the other domains of the CFTR protein will probably result in the reinterpretation of the effect of many other mutations and thereby lead to a reconsideration of the phenotypic effects of the different mutations.

## 5. Materials and methods

### 5.1. Cloning and purification of GST-NBF1 and GST

The NBF1 CFTR cDNA fragment (codons 347–596) generated by primer-directed reverse transcription of RNA from T84 cells and subsequent PCR was cloned in-frame into the *Sma*I site of glutathione *S*-transferase (GST) encoding expression vector pGEX-3X (Pharmacia) and introduced into *Escherichia coli* DH5α cells. Recombinant *E. coli* bacteria were grown at 37°C under vigorous shaking in 20 ml Luria broth supplemented with 0.75 μg/ml ampicillin until the late exponential phase. After dilution with 100 ml medium, fermentation was continued for 1 h and then the expression of the fusion protein was induced by IPTG (0.25 mM final concentration) for a further 3–4 h period. Cells were harvested by centrifugation (2500×*g*; 4°C; 10 min), resuspended in ice-cold 0.1 M phosphate/10% (v/v) glycerol buffer, pH 8, and lysed by sonication (six 5 s pulses at 0°C). The suspension was centrifuged (12 000×*g*; 4°C; 10 min) and the pellet was solubilized in 2 ml denaturation buffer (8 M urea, 2% (v/v) SDS, 20 mM EDTA, 0.06M Tris/HCl, pH 6.8, 10% (v/v) glycerol, 0.05 M DDT). Proteins were separated by preparative single-slot SDS-12% PAGE (13.5×18×0.2 cm gel, 2.2 V/cm, 16 h, 20°C) and visualized by negative staining with $CuCl_2$ [29]. Fusion protein was gel electroluted (5 V/cm, 3–4 h, 4°C) into 2 ml electrophoresis buffer supplemented with 5 mM EDTA for the complexation of copper ions. Ionic

Table 1
Secondary structure elements of CFTR NBF1 and adenylate kinase determined by CD

| Secondary structure elements (%) | NBF1 CFTR | | | Adenylate kinase | | |
|---|---|---|---|---|---|---|
| | α-helix (±5%) | β-sheet (±8%) | random coil (±8%) | α-helix (±5%) | β-sheet (±8%) | random coil (±8%) |
| A: Variation of pH value | | | | | | |
| pH 5 | nd | nd | nd | 45 | 24 | 30 |
| pH 6 | 50 | 17 | 33 | 49 | 24 | 27 |
| pH 7 | 45 | 17 | 38 | 52 | 23 | 28 |
| pH 8 | 26 | 24 | 50 | 51 | 21 | 28 |
| pH 9 | 31 | 18 | 51 | 27 | 14 | 59 |
| B: Variation of ATP concentration at pH 8 | | | | | | |
| 0 mM ATP | 26 | 24 | 50 | 51 | 21 | 28 |
| 0.25 mM ATP | 23 | 39 | 38 | 49 | 22 | 29 |
| 0.5 mM ATP | 30 | 37 | 34 | 57 | 15 | 29 |
| 1 mM ATP | 26 | 38 | 37 | 52 | 23 | 26 |
| 2 mM ATP | 30 | 32 | 38 | 48 | 19 | 33 |
| 4 mM ATP*a* | 8 | 30 | 62 | 57 | 10 | 38 |

nd, not determined.
*a*, absolute error ± (10–20%) because of high absorbance.

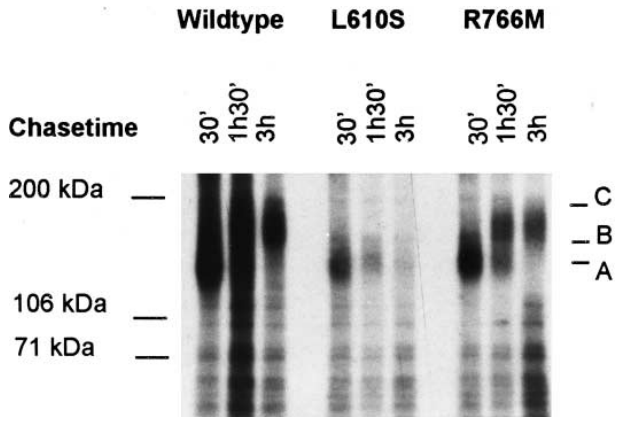


Fig. 3. Representative example of a pulse chase and immunoprecipitation of CFTR from transfectants. COS cells transfected with wild-type CFTR-L610S and CFTR-R766M were metabolically labelled, chased and CFTR was immunoprecipitated and separated on a SDS-PAGE gel. The different maturation forms are indicated: A (= translation product), B (= core-glycosylated protein) and C (= mature CFTR protein).

strength of the protein solution was gradually reduced in 12–18 h intervals by dialysis at 4°C in phosphate buffer supplemented with 1 mM $MgCl_2$/ATP to facilitate refolding and with Dowex resin to absorb SDS (buffer 1: 0.1 M phosphate, 10% (v/v) glycerol; buffer 2: 0.05 M phosphate, 5% (v/v) glycerol; buffer 3: 0.02 M phosphate, 5% (v/v) glycerol; buffer 4: 0.02 M phosphate). The protein solution was stored in 0.02 M phosphate, pH 8 at −70°C until use.

According to spectrophotometric assay of SDS-*p*-rosaniline complexes [30] the purified proteins always contained less than 0.001% SDS. Fusion proteins were cleaved with factor Xa (Boehringer) at a molar ratio of 10:1 to 200:1 in 50 mM Tris-HCl/150 mM NaCl/1 mM $CaCl_2$, pH 7.5 (25°C, 2–3 h) and then separated by SDS-PAGE. Porcine ADK was purchased from Boehringer Mannheim.

### 5.2. CD spectroscopy

Circular dichroism spectra of proteins (concentration range 0.5–1.5 mg/ml) were recorded in 20 mM phosphate buffer at ambient room temperature in 0.01 cm cuvettes (volume 58 μl) in a Jobin-Yvon Dichrograph R.J. Mark III. The band width was always 0.5 nm and the speed 0.5 nm/s (time constant 2 s). After registering the baseline, four consecutive scans ranging from 245 nm down to 184 nm were accumulated. Cumulative spectra were stored in a digital recorder, processed and analyzed numerically in the range 190–243 nm (0.5 nm increments) in terms of α-helices, β-pleated sheets and residual structure content with myoglobin, lysozyme, lactate dehydrogenase, papain and ribonuclease A as reference proteins [31]. The quality of the data analysis could be controlled visually by displaying the superposition of the experimental and theoretical spectra. Since the CD spectra of GST-NBF1 CFTR were identical prior to and after cleavage with factor Xa, the CD spectral increments of GST and NBF1 were assumed to be additive and hence the secondary structure elements of NBF1 were calculated from the spectra of GST and fusion protein.

### 5.3. Expression of wild-type and mutant CFTR proteins

The CFTR.WT coding sequence was excised from the pTG5960 plasmid (Transgene, Strasbourg, France) and cloned into the eukaryotic expression vector pcDNA3 (Invitrogen BV, Leek, The Netherlands). The mutations L610S (tc at 1961), G628R (gc at 2014), L633P (tc at 2030), D648V (at at 2075), T665S (at at 2125) and R766M (gt at 2429) (nucleotide and amino acid assignment according to [2]) were introduced using the Transformer Site-Directed Mutagenesis kit (Clontech, Heidelberg, Germany). COS cells were electroporated with 20 μg plasmid DNA (BioRad Gene Pulser, BioRad Laboratories, Hercules, CA, USA). After 48–72 h cells were labelled during a 30 min pulse with 400 μCi Translabel (ICN Pharmaceuticals, Costa Mesa, CA, USA) and chased in DME F12 (Life Technologies, Merelbeke, Belgium) +10% FCS (Hyclone Laboratories Inc., Logan, UT, USA). The cells were then lysed in ice-cold DIPPA buffer (20 mM Tris, 150 mM NaCl, 1% Na-deoxycholate, 1% Triton X-100, 0.1% SDS, pH 7.4) containing protease inhibitors. After immunoprecipitation with an anti-CFTR monoclonal antibody directed against the C-terminal part of CFTR (Genzyme Diagnostics, Cambridge, MA, CA), the immune complexes were purified on protein A beads (Pharmacia Biotech, Uppsala, Sweden) and loaded on a 4–12% SDS gel (Novex, San Diego, CA, USA). After drying of the gel, the signals were visualized by means of autoradiography.

*Acknowledgements:* We would like to thank Transgene (supported by AFLM), who generously provided the pTG5960 plasmid. Anne Vankeerberghen is a fellow of the Vlaams Instituut voor de Bevordering van het Wetenschappelijk, Technologisch Onderzoek in de Industrie. This work was supported by the Association Française de Lutte contre la Mucoviscidose (AFLM), the Association Française contre les Myopathies (AFM), the Centre de Recherche du Bouchet, the Deutsche Forschungsgemeinschaft (DFG), and the IUAP of the Federal Ministry for Scientific Research (Belgium).

## References

[1] S.C. Hyde, P. Emsley, M.J. Hartshorn, M.M. Mimmack, U. Gileadi, S.R. Pearce, M.P. Gallagher, D.R. Gill, R.E. Hubbard, C.F. Higgins, Nature 346 (1990) 362–365.
[2] J.R. Riordan, J.M. Rommens, B.S. Kerem, N. Alon, R. Rozmahel, Z. Grzelczak, J. Zielenski, S. Lok, N. Plavic, J.L. Chou, M.L. Drumm, M.C. Iannuzzi, F.S. Collins, L.C. Tsui, Science 245 (1989) 1066–1072.
[3] C.J. Ward, S. Omura, R.R. Kopito, J Biol Chem 269 (1994) 25710–25718.
[4] J.P. Abrahams, A.G.W. Leslie, R. Lutter, J.E. Walker, Nature 370 (1994) 621–628.
[5] A.G. Murzin, S.E. Grenner, T. Hubbard, C. Chothia, J Mol Biol 247 (1995) 536–540.
[6] D. Dreusicke, P.A. Karplus, G.E. Schulz, J Mol Biol 199 (1988) 359–371.
[7] U. Egner, A.G. Tomasselli, G.E. Schultz, J Mol Biol 195 (1987) 649–658.
[8] F. Jurnak, Science 230 (1985) 32–36.
[9] C.S. Mimura, S.R. Holbrook, G.F.L. Ames, Proc Natl Acad Sci USA 88 (1991) 84–88.
[10] B. Rost, C. Sander, J Mol Biol 232 (1993) 584–599.
[11] R. Allikmets, B. Gerrard, A. Hutchinson, M. Dean, Hum Mol Gen 5 (10) (1996) 1649–1655.
[12] L. Patard, V. Stoven, B. Gharib, F. Bontems, J.Y. Lallemand, M. De Reggi, Protein Eng 9 (10) (1996) 949–957.
[13] R.L. Dundrack, M. Karplus, J Mol Biol 230 (1993) 543–574.
[14] P. Güntert, W. Braun, K. Wüthrich, J Mol Biol 217 (1991) 517–530.
[15] P. Güntert, K. Wüthrich, J Biomol NMR 1 (1991) 447–456.
[16] Brünger AT. X-PLOR Manual. New Have, CT: The Howard Hughes Medical Institute and Department of Molecular Biophysics and Biochemistry, Yale University, 1988.

[17] J. Kuzensk, A.M. Gronenborn, G.M. Clore, Protein Sci 5 (1996) 1067–1080.
[18] T. Hoof, A. Demmer, M.R. Hadam, J.R. Riordan, B. Tümmler, J Biol Chem 269 (1994) 20575–20583.
[19] J. Zielenski, L.-C. Tsui, Annu Rev Genet 29 (1995) 777–807.
[20] L.S. Havarstein, D.B. Diep, I.F. Nes, Mol Microbiol 16 (2) (1995) 220–240.
[21] D.P. Rich, M.P. Anderson, R.J. Gregory, S.H. Cheng, S. Paul, D.M. Jefferson, J.D. McCann, K.W. Klinger, A.E. Smith, M.J. Welsh, Nature 347 (1990) 358–363.
[22] M.P. Anderson, D.P. Rich, R.J. Gregory, A.E. Smith, M.J. Welsh, Science 251 (1991) 679–682.
[23] R.J. Gregory, D.P. Rich, S.H. Cheng, D.W. Souza, S. Paul, P. Manavalan, M.P. Anderson, M.J. Welsh, A.E. Smith, Mol Cell Biol 11 (1991) 3886–3893.
[24] L.S. Smit, T.V. Strong, D.J. Wilkinson, M. Macek Jr., M.K. Mansoura, D.L. Wood, J.L. Cole, G.R. Cutting, J.A. Cohn, D.C. Dawson, F. Collins, Hum Mol Genet 4 (1995) 269–273.
[25] F.S. Seibert, P. Linsdell, T.W. Loo, J.W. Hanrahan, D.M. Clarke, J.R. Riordan, J Biol Chem 271 (1996) 15139–15145.
[26] S.H. Cheng, R.J. Gregory, J. Marshall, S. Paul, D.W. Souza, G.A. White, C.R. O'Riordan, A.E. Smith, Cell 63 (1990) 827–834.
[27] A. Vankeerberghen, L. Wei, M. Jaspers, B. Nilius, H. Cuppens, J.J. Cassiman, Ped. Pulmonol. Suppl. 13 (1996) 61.
[28] J.R. Riordan, G.M. Rommens, B.-S. Kerem, N. Alan, R. Rozmahel, Z. Gizelczak, J. Zielinski, S. Lok, N. Plavsic, J.-L. Chou, M.L. Drumm, M.C. Iannuzzi, F.S. Collins, L.-C. Tsui, Science 245 (1989) 1066–1073.
[29] C. Lee, A. Levin, D. Branton, Anal Biochem 166 (1987) 308–312.
[30] R. Amons, P.I. Schrier, Anal Biochem 116 (1981) 439–443.
[31] Y.H. Chen, J.T. Yang, H.M. Martinez, Biochemistry 11 (1972) 4120–4131.
[32] P.J. Kraulis, J Appl Crystallogr 24 (1991) 946–950.